

Elucidating the role of many-body forces in liquid water. I. Simulations of water clusters on the VRT(ASP-W) potential surfaces

Nir Goldman

Lawrence Livermore National Laboratory, Chemistry and Materials Science Directorate, L-268, Livermore, California 94551

R. J. Saykally^{a)}

Department of Chemistry, University of California, Berkeley, California 94720-1416

(Received 7 October 2003; accepted 12 December 2003)

We test two new potentials for water, fit to vibration-rotation tunneling (VRT) data by employing diffusion quantum Monte Carlo simulations to calculate the vibrational ground-state properties of water clusters. These potentials, VRT(ASP-W)II and VRT(ASP-W)III, are fits of the highly detailed ASP-W (anisotropic site potential with Woerner dispersion) *ab initio* potential to $(D_2O)_2$ microwave and far-infrared data, and along with the SAPT5*s* (five-site symmetry adapted perturbation theory) potentials, are the most accurate water dimer potential surfaces in the literature. The results from VRT(ASP-W)II and III are compared to those from the original ASP-W potential, the SAPT5*s* family of potentials, and several bulk water potentials. Only VRT(ASP-W)III and the spectroscopically “tuned” SAPT5*st* (with *N*-body induction included) accurately reproduce the vibrational ground-state structures of water clusters up to the hexamer. Finally, the importance of many-body induction and three-body dispersion are examined, and it is shown that the latter can have significant effects on water cluster properties despite its small magnitude. © 2004 American Institute of Physics. [DOI: 10.1063/1.1645777]

I. INTRODUCTION

Given the recent determinations of accurate and highly detailed two-body potentials for water from the spectroscopic data available for the water dimer,^{1–4} in conjunction with high level *ab initio* results,^{5–7} we are presented with an opportunity to explore the intricacies of intermolecular forces governing the liquid and solid phases of water. In a recent paper, Hodges *et al.* calculate the total *ab initio* interaction energies for the water trimer, tetramer, and pentamer and dissect them into their respective *N*-body components.⁸ The results show that the two-body forces comprise approximately 75% of the total energy, the three-body terms approximately 20%, and the four-to-five-body terms the remaining 5%. In a more detailed paper, Ojåme and Hermansson performed a similar analysis of many-body forces operative in chains of water molecules up to the heptamer, in ring structures up to the pentamer, and in a tetrahedral pentamer.⁹ These calculations, performed at the second-order Møller–Plesset (MP2) level, yield some striking insights. In both the water heptamer chain and the pentamer ring structure, they find that two-body forces account for over 80% of the total interaction energy, and that two- and three-body terms together account for over 99%. In the tetrahedral pentamer, which closely resembles the average liquid and normal ice structures, they find that the two-body energy constitutes over 87% of the total interaction energy, and the two- and three-body terms together comprise approximately 99.6%. In all cases, the total energies of larger

clusters are rapidly converging and are essentially fully converged by accounting for only the two- and three-body terms. Hence, description of the pairwise interaction appears to be of paramount importance for constructing a complete molecular (i.e., nonempirical) description of the liquid.

Two of the most accurate water dimer potentials obtained to date are the recently determined vibration-rotation-tunneling (VRT)(ASP-W)II and III water dimer intermolecular potential-energy surface (IPS).² These are the second and third fittings, respectively, of Millot and Stone’s ASP-W *ab initio* potential¹⁰ to $(D_2O)_2$ intermolecular VRT transitions. The dimer tunneling splittings from hydrogen bond rearrangements and the intermolecular vibrational frequencies provide a highly sensitive probe of the complex water intermolecular potential-energy surface (IPS),¹¹ and such measurements have been made extensively by our laboratory.^{12–14} The ASP-W potential has 72 parameters, corresponding to electrostatic interactions, two-body exchange-repulsion, two-body dispersion, and many-body induction, but it was found previously that accurate fits to the data could be produced by fitting four to six of the 22 exchange-repulsion parameters.¹⁵ Thus the VRT(ASP-W)II IPS was created by fitting four of the exchange-repulsion parameters in ASP-W (Ref. 10) to 25 experimentally derived $(D_2O)_2$ microwave and far-infrared (IR) transitions, and the VRT(ASP-W)III potential was generated by fitting six of the exchange-repulsion parameters to an additional five far-IR vibrational band origins. VRT(ASP-W)II and III constitute substantial improvements over the original VRT(ASP-W) potential,² although van der Avoird and co-workers have obtained one of comparable quality for the $(H_2O)_2$ isotopomer

^{a)} Author to whom correspondence should be addressed. Electronic mail: saykally@uclink4.berkeley.edu

by “tuning” an *ab initio* potential derived from symmetry adapted perturbation theory (SAPT),³ discussed below.

Diffusion quantum Monte Carlo (DMC, discussed below) calculations on the ASP-W IPS have shown that induction is by far the most important many-body term in the total cluster interaction energy,¹⁶ which was also confirmed by *ab initio* calculations.¹⁷ Considering the fact that the VRT(ASP-W) dimer potential explicitly contains many-body induction in the form of electric multipoles and a tensorial polarizability, this IPS may actually be closer to a “universal” model for water than one would anticipate. However, it is important to note that Refs. 8 and 9 study relatively small systems and thus neglect long-range correlations which are present within the liquid (cf., Ref. 18). Hence it is possible that the total interaction energy of liquid water may not be as rapidly convergent as that for clusters. It is the goal of this and a forthcoming paper to explore the details of these subtle correlations that are present in the liquid.

Given its accuracy for describing the dimer, the next logical step is to test the VRT(ASP-W) IPS family of spectroscopic potentials in quantum simulations of higher clusters. Much spectroscopic data exist for larger clusters, particularly ground-state properties of up to the hexamer.^{19–24} We can thus simulate larger clusters with these potentials and compare results to the data in order to further test the validity of our IPS models. Diffusion quantum Monte Carlo is a useful simulation technique for such purposes.^{25–30} It is a fully quantum-mechanical technique with a computational cost that scales favorably with cluster size and potential complexity. Furthermore, it is an excellent complement to *ab initio* calculations because directly observable vibrationally averaged properties are calculated, rather than just the (unobservable) equilibrium properties. Quack and Suhm have utilized DMC extensively in similar studies of (HF)_n clusters^{31–35} and have determined highly accurate potentials for HF aggregates.

The starting point of a DMC simulation is the time-dependent Schrödinger equation, which is rewritten in imaginary time and thus becomes isomorphic with the diffusion equation. Consequently, the eigenstate of interest can be simulated via random diffusion. The original formulation for DMC was developed by J. Anderson in order to study one- to four-electron systems.^{36,37} There are a number of articles reviewing DMC, and thus the technique will not be discussed herein. For further information, the reader is in particular directed to the excellent review article by Suhm and Watts.³⁸ Further specific information on DMC simulations of water clusters can be found in a series of papers by Gregory and Clary.^{25–29} All of the IPS used in the cluster calculations herein use a “frozen monomer” approximation, in which intramolecular degrees of freedom are not explicitly included in the calculation. Such IPS will be henceforth referred to as rigid potentials. Since intermolecular degrees of freedom are treated separately from intramolecular vibrations, and are of a lower frequency, a larger time step can be used in the rigid body simulations. A simple method for treating monomers as rigid bodies has been developed by Buch and others,^{39,40} called RBDMC, and again the reader is referred to the those references for further information. There are limitations to

diffusion quantum Monte Carlo, however, primarily in its inability to calculate excited states. Considerable recent progress has been made in that area and the reader is directed to the listed references for details.^{26,41,42} Nonetheless, current excited state DMC algorithms are complicated and difficult to implement, and their ability to simulate excited states is still being assessed. Therefore we restrict our present interests to the nodeless ground state.

In the following, we present vibrational ground-state DMC results for the water dimer through hexamer for a variety of different potential-energy surfaces. Results from VRT(ASP-W)III are compared to those from experiment and ASP-NB (*N*-body) created by Gregory and Clary²⁸ by adding an approximate form for three-body dispersion (Axilrod–Teller–Muto triple-dipole interaction, discussed below) to the original ASP-W potential of Millot and Stone.¹⁰ Comparisons between VRT(ASP-W)II and III are made in order to assess the effects of our fits on vibrational ground states of water clusters greater than the dimer. Due to the high level of accuracy attained for the dimer⁶ and trimer,⁷ simulation results from the SAPT5s family are presented as well. Additional comparisons are made to SPC/E (extended simple point charge),⁴³ and PSPC (polarizable simple point charge),⁴⁴ to investigate how the properties of these bulk water potentials differ from those of the gas phase models in terms of cluster simulations. Based on comparison to MP2 results from Ref. 28 and to experimental results, the effectiveness of including induction as the only many-body force is evaluated. The effects of three-body dispersion in DMC simulations is then quantified.

II. GROUND-STATE PROPERTIES OF WATER CLUSTERS: COMPARISON TO EXPERIMENTS

In all RBDMC simulations performed here, a population of 1000 walkers was used, and these comprised an equilibration stage followed by a propagation stage over which properties were averaged. For the dimer, trimer, and tetramer, equilibrium periods of 2000 time steps of 40 a.u. were used, while those for the pentamer and hexamer were longer, consisting of 6000 time steps at 40 a.u. This was necessary due to the high dimensionality of the IPS used in our simulations and the existence of numerous local minima and potential barriers. The ground-state eigenvalues were obtained by averaging E_R over the entire propagation stage of 15 000–20 000 time steps of magnitude 20 a.u., and histograms of configurations were used to calculate the inertial tensor and hence the moments of inertia and rotational constants.

In order to completely characterize the potential-energy surfaces, searches for local minima were performed using the eigenvector following method, available in the ORIENT 4.4 program.⁴⁵ Starting geometries were taken from RBDMC simulations or were generated randomly. An exhaustive search for minima was too time consuming, considering the large number of local minima Gregory and Clary found for the pentamer and hexamer,²⁸ so searches for structures already identified by Gregory and Clary with the ASP-NB IPS (discussed below) that were deemed important were performed instead. To distinguish these structures from vibrational ground-state structures, we labeled the equilibrium

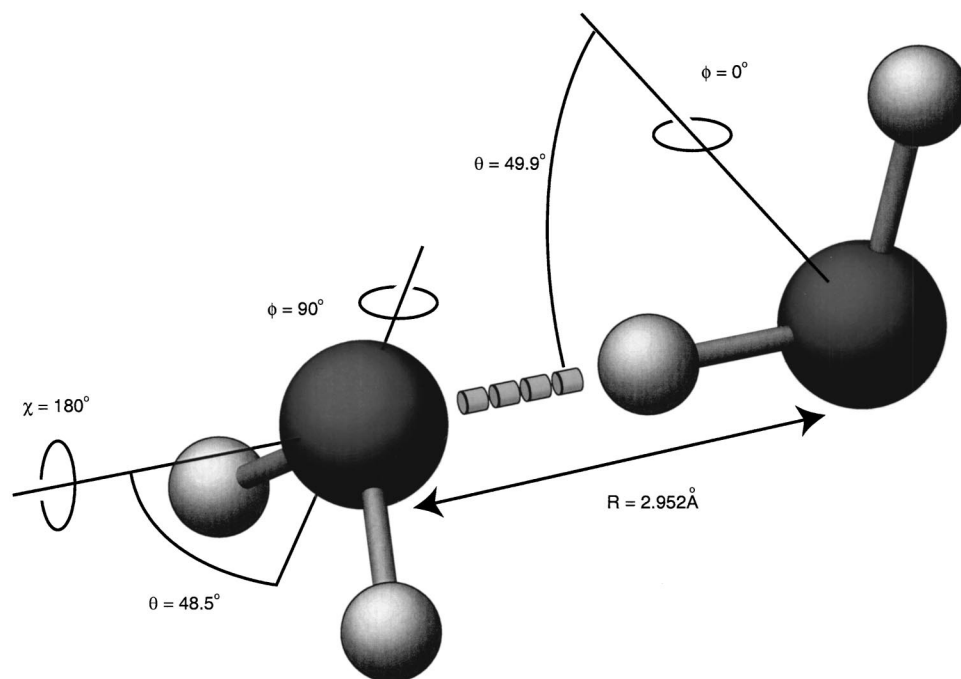


FIG. 1. Equilibrium structure of the water dimer obtained from VRT(ASP-W)III.

structures determined by ORIENT 4.4 as **ES**, and the vibrational ground-state structures determined from DMC as **VGS**.

When examining dissociation energies D_0 of local minima structures, the constraint suggested by Gregory and Clary was used to keep the simulation in the local minimum of interest.²⁸ In such a quantum simulation, collapse to a lower energy structure is usually caused by a single walker moving out of the given minimum and hence causing the entire walker population to drift out of the well. To prevent this, one can simply delete any walker that is of lower energy than D_e of the local minimum being studied, forcing the simulation to remain within that particular local minimum.

Comparisons are made to the D_e and D_0 values found by Gregory and Clary, in Ref. 28, both from RBDMC and *ab initio* calculations, the former performed with the ASP-NB potential. This potential was derived by taking the ASP-W potential,¹⁰ which includes many-body induction, and adding three-body dispersion via a simple Axilrod–Teller–Muto (ATM) triple-dipole term.^{46,47} Their *ab initio* calculations were performed using second-order Møller–Plesset (MP2) perturbation theory and a double- ζ plus polarization basis, and they computed D_0 values for clusters up to and including the tetramer from the MP2 harmonic frequencies.

RBDMC calculations were performed on the original ASP-W and VRT(ASP-W)II and III. VRT(ASP-W)III emerged as the best of these models, both because it was fit to the largest set of experimental data, and via comparison of ground-state structures of the dimer through hexamer. In terms of $(\text{H}_2\text{O})_2$, VRT(ASP-W)II and III are quite similar, as evidenced by the computed $(\text{H}_2\text{O})_2$ properties calculated. However, as will be shown below, fitting VRT(ASP-W)III to this slightly larger parameter and data set produced an IPS

that is not only a better dimer potential, but one that is also a better model for larger clusters.

Calculations have also been performed on the SAPT family of potentials for the water dimer, as mentioned above. The SAPT5s *ab initio* pair potential was developed a few years ago and was shown to have near-spectroscopic accuracy,^{3,4,6} but it is strictly a pair potential and cannot be used to accurately simulate clusters larger than the dimer.

In a more recent publication,⁷ Mas *et al.* extended the SAPT5s formalism to include three-body forces by performing supermolecular self-consistent field (SCF) and three-body SAPT calculations for 7533 trimer geometries. The nonadditive energies from these calculations were then fit to an analytic formula motivated by the SAPT analysis and containing representations of short-range exchange and damped induction contributions. This form of three-body exchange and induction was then combined with the SAPT5s dimer potential to form the SAPT5s+3B IPS, which was tested extensively for $(\text{H}_2\text{O})_3$ and $(\text{D}_2\text{O})_3$ equilibrium structure and energetics, and used to simulate the liquid.⁴⁸ To the best of our knowledge, SAPT5s+3B is the only existing 12-dimensional (12D) (i.e., including all intermolecular coordinates, with frozen monomers) nonadditive *ab initio* potential for the water trimer with explicit three-body exchange terms. However, SAPT5s+3B by itself omits a description of the $N > 3$ -body forces acting within clusters, viz. $N > 3$ -body induction, which are the largest N -body forces.

In order to simulate clusters larger than trimer, we included N -body induction in SAPT5s+3B in a similar fashion to Mas *et al.*,⁴⁸ viz. by calculating the N -body induction from VRT(ASP-W)III and subtracting off the total three-body and total two-body induction. Hence the two-body and three-body induction used in these simulations was per-

TABLE I. Well depths (D_e) and dissociation energies (D_0) of the dimer as described in the text.

Model	$(\text{H}_2\text{O})_2$	
	D_e (cm^{-1})	D_0 (cm^{-1})
MP2 ^a	-1773	-910
ASP-NB ^a	-1641	-981
VRT(ASP-W)II	-1544	-1055
VRT(ASP-W)III	-1678	-1080
SAPT5 _s	-1699 ^b	-1067 ^c
PSPC	-3125	-901
SPC/E	-4499	-1664

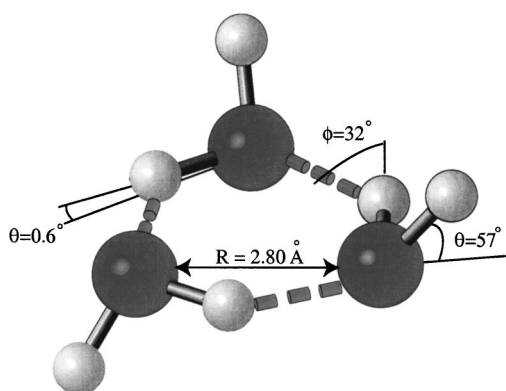
^aResults from Gregory and Clary (Ref. 28).

^bMas *et al.* (Ref. 6).

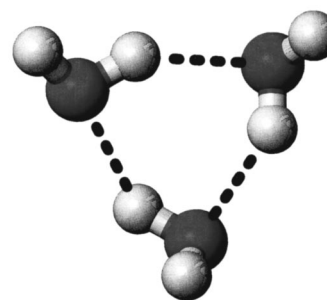
^cGroenenboom *et al.* (Ref. 4).

formed on the SAPT5_s+3B potential, and the $N>3$ -body induction was calculated on VRT(ASP-W)III. We called this N -body form of the potential, SAPT5_s+NB(ASP). For further clarification, the dimer simulations were performed on SAPT5_s, the trimer on SAPT5_s+3B, and the tetramer through hexamer on SAPT5_s+NB(ASP). Unfortunately, the repeated calculation of iterated induction via VRT(ASP-W)III made all simulations with SAPT very costly. Hence calculations were performed for H₂O clusters only. Also, the three-body forces in the SAPT code were not compatible with the ORIENT 4.4 software. Hence the only equilibrium data given herein are those already reported for the dimer⁶ and trimer.⁷ As stated above, there also exists a fitted “tuned” form of SAPT5_s called SAPT5_{st}, which has an even higher degree of spectroscopic accuracy for (H₂O)₂. However, since the recent publications of Mas *et al.*^{7,48} deal exclusively with the untuned SAPT5_s potential, and due to the high computational cost of including N -body induction, we decided to limit the RDMC simulations with SAPT5_{st} to the pentamer and hexamer. Both of these clusters are crucial for determining the accuracy of the IPS, and SAPT5_s+NB(ASP) has proven accurate only up through the pentamer (Sec. II D). The N -body form of SAPT5_{st} was called SAPT5_s+NB(ASP-T), in order to readily distinguish it from the untuned SAPT5_s IPS.

Simulations were also performed on the SPC/E (Ref. 43) and PSPC (Ref. 44) models for liquid water. SPC/E is a popular and reasonably good model for room temperature water at normal density.⁴⁹ PSPC is one of several polarizable potentials with the same pairwise functional form as SPC/E (cf. Ref. 50). Its model for polarizability is fairly crude, since it ascribes atomic polarizabilities to the oxygen and hydrogens of the water monomer, rather than allowing for anisot-



(a) (uud)



(b) (uuu)

FIG. 2. (H₂O)₃ equilibrium structures from VRT(ASP-W)III. *Ab initio* equilibrium structural properties of the (uud) structure are given in Ref. 56.

ropy via a second rank polarizability tensor for each monomer. It is not as accurate as SPC/E in terms of the total liquid dipole moment and diffusion constant at standard thermodynamic conditions, but it does accurately reproduce the gas phase water dimer dipole moment and is able to produce reasonable radial distribution functions for the liquid that clearly reflect tetrahedral structure. Consequently, because it contains induction terms, it should act as a good “transition” potential in that it would serve as a reasonable model for bridging the gas and bulk phases. In particular, we thought it would be interesting to see at what cluster size, if any, SPC/E, PSPC, and our gas-phase cluster models begin to exhibit the same structural properties, and perhaps indicate when gas-phase clusters might truly begin to mimic the bulk.

A. (H₂O)₂

The water dimer structure is shown in Fig. 1, the values of D_e and D_0 are shown in Table I, and the rotational constants are given in Table II.

TABLE II. Vibrationally averaged dimer rotational constants.

(H ₂ O) ₂	VRT(ASP-W)II	VRT(ASP-W)III	SAPT5 _s ^a	PSPC	SPC/E	Expt. ^b
A (GHz)	232.01	230.36	207.76	219.53	222.549	227.6
B (GHz)	6.01	5.99	$\frac{B+C}{2} =$	6.16	6.752	$\frac{B+C}{2} =$
C (GHz)	5.95	5.92	6.13	6.07	6.647	6.16

^aGroenenboom *et al.* (Ref. 4).

^bExperimental results from Ref. 55, pp. 133 and 170.

TABLE III. D_e and D_0 for the lowest two trimer potential minima. Results for both the (*uud*) and (*uuu*) structures are shown. The value of D_0 for (*uuu*) could not be calculated with local minima constraints (see text for discussion).

(H ₂ O) ₃ Model	(<i>uud</i>)		(<i>uuu</i>)	
	D_e (cm ⁻¹)	D_0 (cm ⁻¹)	D_e (cm ⁻¹)	D_0 (cm ⁻¹)
MP2 ^a	-5501	-3008	-5214	-2919
ASP-NE ^a	-5626	-3509	-5297	
VRT(ASP-W)II	-5615	-3619	-5432	
VRT(ASP-W)III	-5432	-3557	-5307	
SAPT5 _s +3B	-5287 ^b	-3610	-5090 ^b	
PSPC		-2601		
SPC/E		-2279		

^aGregory and Clary (Ref. 28).

^bMas *et al.* (Ref. 7).

It is important to note in Table I that the MP2 harmonic D_0 energy is much higher than most of the other predictions (excluding PSPC), clearly evidencing the large anharmonicity of the dimer vibrations. The rotational constants from VRT(ASP-W)II and III are both within a few percent of experimental values. The published results for SAPT5_s yield a value for *A* that is approximately 9% too small, but values for *B* and *C* that are very close to (within less than 1%) experimental values. SPC/E yields *B* and *C* rotational constants that are much too high due to the fact that the $\langle R_{OO} \rangle$ value that it predicts (2.82 Å) is much shorter than the experimental dimer value (2.99 Å). PSPC gives an $\langle R_{OO} \rangle$ value (2.99 Å) and rotational constants that compare well to experiments. However, it gives a value of D_0 that is significantly higher than all other potentials [approximately 17% above that from VRT(ASP-W)III], including the MP2 surface. Also, both SPC/E and PSPC have values of D_e that are vastly lower than all other IPS that were tested.

B. (H₂O)₃

The global minimum in all potentials tested is the (*uud*) structure (Fig. 2) wherein two of the free hydrogens point up from the [OOO] plane while the third points downward. The first local minimum in all potentials is the (*uuu*) structure (Fig. 2), wherein all three free hydrogens point upward from the [OOO] plane. The detailed structure of the global minimum is consistent with experimental results, as reviewed recently by Keutsch *et al.*⁵¹

The values for D_e and D_0 are shown in Table III. VRT(ASP-W)II continues to compare well to version III, yielding values of D_e and D_0 that are all within a few percent. The values of D_e and D_0 for SAPT5_s+3B are 3% and 1.5% lower, respectively, than those for VRT(ASP-W)III. It is interesting to note that the value of D_0 for SPC/E is significantly higher than those of the other potentials, whereas it was instead much lower for the dimer. This is most likely due to the highly nonlinear hydrogen bonding geometry obtained in the trimer. D_0 for PSPC is now approximately 27% higher than that of VRT(ASP-W)III, indicating that it fails to model some of the cooperative effects present in the VRT(ASP-W)III trimer, at least in this geometry.

Rotational constants for (H₂O)₃ and (D₂O)₃ for all potentials are shown in Table IV. Experimental rotational constants measured for both (H₂O) and (D₂O)₃ confirm that the (*uud*) structure is the VGS. As expected, the rotational constants of the VGS correspond to an oblate top ($A = B > C$). It is important to note that this symmetric VGS is partially due to the facile “flipping” motion of the down (*d*), or free hydrogen.^{1,52} The flipping motion results in the (*d*) hydrogen spending an equal amount of time above and below the [OOO] plane, and thus the asymmetric equilibrium structure averages to the symmetric oblate top. This tunneling motion is not taken into account during the averaging stage of our simulations because the calculated moments of inertia were pre-ordered from greatest to smallest in magnitude, in order to simplify the averaging process. Hence the average value of *A* and *B* yielded from each IPS is highly relevant to the current discussion. Thus, the calculated rotational constants of the VRT(ASP-W)III D₂O trimer correspond reasonably well, and the average of *A* and *B* are within approximately 6% of experiment. Interestingly, the SAPT5_s+3B potential yielded rotational constants that are nearly identical to those from VRT(ASP-W)III. The ASP-NB IPS is able to more closely predict the oblate top as a ground state structure, although the calculated values of *A* and *B* are approximately 20% too high. This is surprising, considering that ASP-NB was not fit to experimental data and the included three-body dispersion forces are generally considered small enough to neglect.⁸ However, it should be noted that the average of the *A* and *B* rotational constants of VRT(ASP-W)III is much closer to the actual experimental result.

Finally, effort was made to constrain the DMC simulation into the (*uuu*) potential well. As shown in Table III, all

TABLE IV. Vibrationally averaged (H₂O)₃ and (D₂O)₃ rotational constants for (*uud*).

(H ₂ O) ₃	VRT(ASP-W)II	VRT(ASP-W)III	SAPT5 _s +3B	PSPC	SPC/E	Expt. ^a
<i>A</i> (GHz)	7.04	6.84	6.87	6.74	6.614	6.646
<i>B</i> (GHz)	5.85	5.68	5.72	5.49	5.324	6.646
<i>C</i> (GHz)	3.24	3.15	3.16	3.05	2.973	3.513 (AF)
(D ₂ O) ₃	VRT(ASP-W)III		ASP-NB		Expt. ^a	
<i>A</i> (GHz)	5.942		6.886		5.796	
<i>B</i> (GHz)	4.997		6.769		5.796	
<i>C</i> (GHz)	3.167		3.534		AF	

^aExperimental results are from Ref. 52. The value of *C* could not be determined experimentally and hence was arbitrarily fixed (AF).

TABLE V. D_e and D_0 for the (*udud*) tetramer structure, and D_e for the (*uudd*) and (*uuud*) structures. The VGS for SPC/E was found to be (*uudd*), as noted.

$(\text{H}_2\text{O})_4$ Model	<i>(udud)</i>	
	D_e (cm^{-1})	D_0 (cm^{-1})
MP2 ^a	-10 016	-6148
ASP-NB ^a	-10 058	-6412
VRT(ASP-W)II	-10 093	-6732
VRT(ASP-W)III	-10 052	-6750
SAPT5 _s +NB(ASP)		-6338
PSPC		-4486
SPC/E (<i>uudd</i>)		-3981

$(\text{H}_2\text{O})_4$ Model	D_e (cm^{-1})			
	<i>(uudd)</i>	<i>(uuud)</i>	cage	C_s
MP2 ^a	-9715	not a minimum	N/A	-7575
ASP-NE ^a	-9683	-9630	N/A	-8211
VRT(ASP-W)II	-9729	-9717	-8637	-7668
VRT(ASP-W)III	-9709	-9687		

^aGregory and Clary (Ref. 28). The cage results for ASP-NB and the MP2 calculations are marked as N/A because the cage structure collapsed to (*udud*) in both cases. The results for the cage and C_s tetramer of VRT(ASP-W)III are left blank because corresponding stable local minima could not be found.

simulations eventually collapsed into the (*udud*) ground state. This is consistent with the findings of Gregory and Clary,²⁸ and is likely due to the aforementioned low potential barrier for flipping of the down (*d*) hydrogen.

C. $(\text{H}_2\text{O})_4$

It is well established^{1,28} that the VGS for the tetramer is the cyclic (*udud*) structure, shown in Fig. 3(a). However, other stable low-energy structures are possible, as demonstrated by a search for local minima on the IPS. Figures 3(b)–3(e) show the lowest-lying structures found by us and by Gregory and Clary.²⁸ Excluding SPC/E, all of the IPS tested here showed the (*udud*) structure as the global minimum, consistent with most previous work. On the VRT(ASP-W)III IPS, the only additional minima found were the cyclic (*uudd*) and (*uuud*) structures.

Results of ORIENT 4.4 and RBDMC calculations are shown in Table V. As stated in the Introduction, the SAPT5_s code was not compatible with the ORIENT 4.4 software; hence the local minima of SAPT5_s+NB(ASP) were not explored. Excluding SPC/E and PSPC, all of the potentials show good agreement with the MP2 D_e and D_0 results, and D_0 from

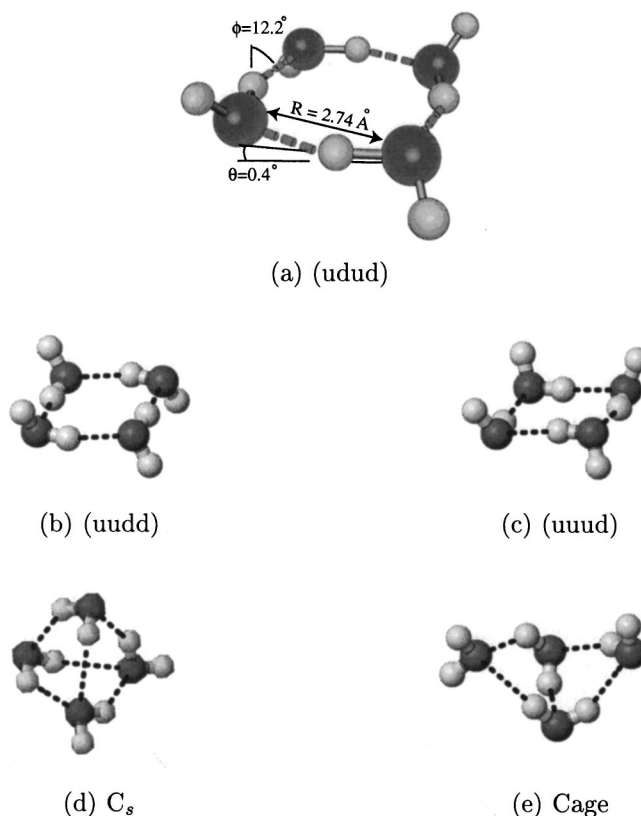


FIG. 3. Equilibrium structures for the water tetramer obtained from the original ASP-W. *Ab initio* equilibrium structural properties of the (*udud*) structure are shown (from Ref. 56).

SAPT5_s+NB(ASP) was 6.5% lower relative to VRT(ASP-W)III. As Gregory and Clary point out, for both (*uudd*) and (*uuud*) there are two cis- and two trans-type interactions, which explains why these structures are consistently similar in energy. In the (*udud*) structure, there are four trans-type interactions, which explains why it is lower in energy. The SPC/E result is particularly distant from other calculations, with a D_0 that is approximately 40% higher and a VGS of (*uudd*). The high VGS dissociation energy results from the fact the tetramer also has highly nonlinear hydrogen bonds, not well described by this bulk liquid model. PSPC predicts the (*udud*) structure as the VGS, but has a D_0 approximately 34% higher than that of VRT(ASP-W)II or III.

We attempted to calculate D_0 for the (*uudd*) and (*uuud*) structures on the VRT(ASP-W)III surface and found that they collapsed to the more stable (*udud*) structure. This

TABLE VI. Rotational constants for (*udud*) of the tetramer.

$(\text{H}_2\text{O})_4$	VRT(ASP-W)II	VRT(ASP-W)III	SAPT5 _s +NB(ASP)	PSPC	SPC/E
A (GHz)	3.70	3.64	3.60	3.52	3.450
B (GHz)	3.17	3.11	2.99	2.88	2.817
C (GHz)	1.75	1.72	1.68	1.61	1.576
$(\text{D}_2\text{O})_4$	VRT(ASP-W)III		ASP-NB		Expt. ^a
A (GHz)	3.183		3.063		3.080
B (GHz)	2.765		3.063		3.080
C (GHz)	1.536		1.583		AF

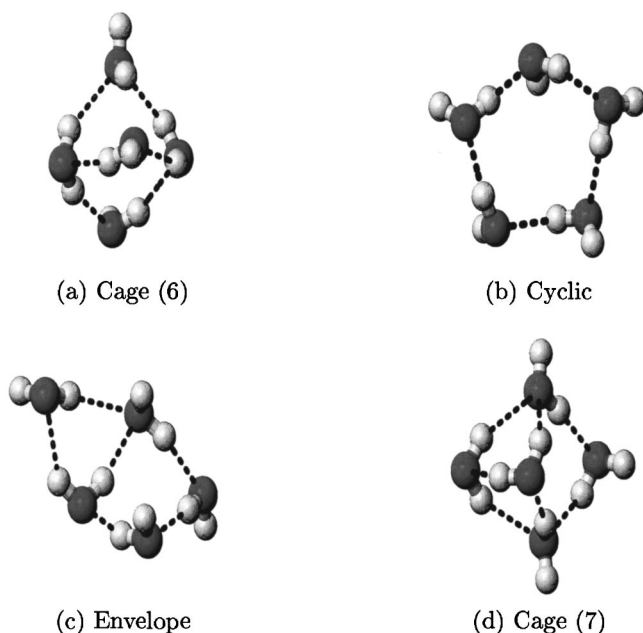


FIG. 4. Equilibrium structures for the water pentamer, obtained from ASP-W.

is consistent with Gregory and Clary's findings, where they point out that they expect the above to happen since the flipping of a hydrogen should be very facile. Our inability to locate a cage minimum is also consistent with their results, since they found the cage structure to collapse to (*udud*) for both ASP-NB and MP2. However, they were able to locate the C_5 equilibrium structure on both surfaces, whereas we could not find this structure on VRT(ASP-W)III.

Vibrationally averaged rotational constants for all global minima are shown in Table VI, and comparison is made to experimental results for $(D_2O)_4$. Rotational constants for $(H_2O)_4$ have not yet been measured at the time of this publication. Interestingly, the SAPT potential once again yields rotational constants that are very similar to those from VRT(ASP-W)III, with the value of B deviating the most, but by only approximately 4%. In terms of $(D_2O)_4$, ASP-NB results are quite close to the experimental properties of an oblate top. VRT(ASP-W)III performs very well, with the average of A and B differing from experiment by less than 10%. Again, calculations were not performed on SAPT5s + NB(ASP) for $(D_2O)_4$ due to the high cost of the simulation.

D. $(H_2O)_5$

There have been a number of structural studies of the water pentamer using various empirical potentials, as discussed by Gregory and Clary.²⁸ Most of these studies predict a low-energy cyclic structure, although other structures are also found to be the global minimum, and all studies predict several structures of similar energy. The general belief that the cyclic structure is the global minimum initiated a number of studies on this particular structure, which was characterized experimentally by Liu *et al.*²⁰

Contrasting the cases of the trimer and tetramer, several local minima were found on the VRT(ASP-W)III potential.

TABLE VII. D_e and D_0 for the $(H_2O)_5$ minimum-energy structures.

$(H_2O)_5$ model	Ground state	
	D_e (cm^{-1})	D_0 (cm^{-1})
MP2 (cyclic)	-13 341	
ASP-NB [cage (6)]	-13 179	-8571
VRT(ASP-W)II (envelope)	-13 264	-8907
VRT(ASP-W)III (cyclic)	-13 399	-9081
SAPT5s + NB(ASP) (cyclic)		-8522
SAPT5s + NB(ASP-T) (cyclic)		-8734
PSPC (cyclic)		-6010
SPC/E (tetrahedron)		-9134

^a D_0 for the MP2 surface was not calculated by Gregory and Clary (Ref. 28).

Our energy minimization searches were limited to the three lowest lying ES's, shown in Fig. 4. The cage (6) structure is differentiated from the cage (7) structure in that it contains a network of six hydrogen bonds instead of seven. It is lower in energy because, although it has fewer hydrogen bonds, the ES is not as contracted and thus can achieve more nearly linear hydrogen bonding, very close to the ideal hydrogen bond geometry. The envelope is made up of a (*udud*) tetramer structure with an additional monomer hanging off to one side and out of the [*OOOO*] plane.

Investigation of the global minima of the pentamer potential-energy surfaces, shown in Table VII, proved to be very interesting, as the potential models predict a variety of different VGS. The correct cyclic pentamer VGS was predicted by MP2 surface, VRT(ASP-W)III, SAPT5s + NB(ASP) and SAPT5s + NB(ASP-T), and these four potentials contain minimal differences in terms of the ground-state and equilibrium properties. The predicted values of D_e from the MP2 calculations and VRT(ASP-W)III are within 60 cm^{-1} of each other, which is remarkably close. The value of D_0 from SAPT5s + NB(ASP) deviates from that of

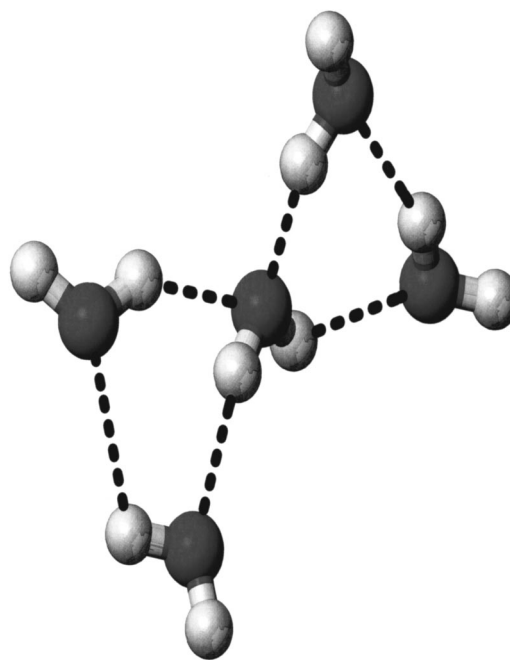


FIG. 5. $(H_2O)_5$ VGS for SPC/E, an icelike pentamer or tetrahedron.

TABLE VIII. D_e and D_0 for all investigated structures of the pentamer. RBDMC simulations with VRT(ASP-W)II and III constrained to the cage (6) minimum collapsed to their respective ground state. Cage (7) structures could not be located on the VRT(ASP-W)II and III potential surfaces.

(H ₂ O) ₅ model	Envelope		Cyclic		Cage (6) D_e (cm ⁻¹)
	D_e (cm ⁻¹)	D_0 (cm ⁻¹)	D_e (cm ⁻¹)	D_0 (cm ⁻¹)	
MP2	-12 572		-13 341		-12 308
ASP-NB	-13 072	-8414	-13 124	-8389	-13 179
VRT(ASP-W)II	-13 264	-8907	-13 417		-12 916
VRT(ASP-W)III	-13 194	-8929	-13 399	-9081	-12 741

VRT(ASP-W)III by +6.2%, and that from SAPT5_s+NB(ASP-T) by +3.8%. Again, our DMC simulations of the “tuned” SAPT5_s+NB(ASP-T) were limited to pentamer and hexamer, due to the high computational cost of including N -body induction in the simulation, and because recent trimer and liquid studies of the IPS deal exclusively with the untuned form of the potential.

ASP-NB, VRT(ASP-W)II, PSPC and SPC/E all predict a wide variety of vibrational ground-state structures, other than the cyclic structure. ASP-NB predicts the cage (6) structure for the global minimum for both D_e and D_0 , which is somewhat surprising, considering how remarkably well this IPS performed for the dimer, trimer, and tetramer. Comparison of VRT(ASP-W)II to VRT(ASP-W)III is also interesting, since VRT(ASP-W)II has a global minimum of the cyclic structure but predicts the envelope as the vibrationally averaged ground-state. Noting that an equivalent basis set was used for each fit, this demonstrates the extreme sensitivity of the IPS to subtle details. The PSPC potential predicts the cyclic structure as the VGS, although once again the value of D_0 is considerably higher than all of the other surfaces, approximately 34% in this case. SPC/E predicts the tetrahedral-like structure for the VGS, as shown in Fig. 5. Given its tetrahedral parametrization, this is not particularly surprising. The structure shown is taken from a snapshot of a walker at the very end of an RBDMC simulation. The fact that the pentamer accommodates this preferred structure, with linear hydrogen bonds, undoubtedly accounts for the large drop in D_0 in going from the tetramer to the pentamer.

Energetics of pentamer structures are summarized in Table VIII, excluding those from PSPC and SPC/E, which again were not tested as extensively due to their inaccuracy in predictions of pentamer ground-state properties, and

SAPT5_s+NB(ASP) and SAPT5_s+NB(ASP-T), due to their incompatibility with ORIENT 4.4. Comparison of the MP2 results for the envelope and cage (6) to the other surfaces shows that the MP2 values of D_e are a small but significant amount higher—5% higher and 3% higher, respectively, compared to VRT(ASP-W)III. Such small differences can prove significant, as highlighted by comparison of results from VRT(ASP-W)II and III; their values for the ground-state D_e and D_0 are within 1% of each other, and yet each predicts different ground-state structures.

Vibrationally averaged ground-state rotational constants for (H₂O)₅ are shown in Table IX, and comparison is made to experimental results for (D₂O)₅. [Again, rotational constants for (H₂O)₅ have not been measured at the time of this publication.] Also, the rotational constants from SAPT5_s-NB(ASP) and SAPT5_s-NB(ASP-T) are fairly close (within 10%) to those from VRT(ASP-W)III. The cyclic structure rotational constants of ASP-NB were reported by Gregory and Clary, and although they do not predict it as the VGS, they do predict rotational constants from simulations constrained to the cyclic structure potential minimum that are quite close to experiment. VRT(ASP-W)III also does reasonably well, as the average of A and B is within 15% of experimental values.

E. (H₂O)₆

There is significant theoretical interest in the hexamer, since it is the first experimentally characterized water cluster VGS that has a three-dimensional (3D) arrangement of monomer center of masses. Experimental results²¹ have indicated that the ground-state structure is most likely the cage,

TABLE IX. Vibrationally averaged ground-state rotational constants for the pentamer.

(H ₂ O) ₅	VRT(ASP-W)II ^a	VRT(ASP-W)III	SAPT5 _s +NB(ASP)	SAPT5 _s +NB(ASP-T)	PSPC	SPC/E ^b
A (GHz)	2.389	2.280	2.05	2.05	1.995	3.321
B (GHz)	1.901	1.731	1.72	1.75	1.623	1.073
C (GHz)	1.668	1.074	0.98	0.98	0.920	0.919
(D ₂ O) ₅	VRT(ASP-W)III		ASP-NB ^a		Expt. ^b	
A (GHz)	1.832		1.739		1.750	
B (GHz)	1.602		1.739		1.750	
C (GHz)	0.894		0.849		AF	

^aRotational constants of the envelope structure.

^bRotational constant of the tetrahedral pentamer.

TABLE X. D_e and D_0 for the prism, cage, and cyclic hexamer structures. The book structure for VRT(ASP-W)II was not investigated.

$(\text{H}_2\text{O})_6$ model	Prism		Cage		Cyclic D_e (cm^{-1})	Book D_e (cm^{-1})
	D_e (cm^{-1})	D_0 (cm^{-1})	D_e (cm^{-1})	D_0 (cm^{-1})		
MP2	-16 137		-16 088		-16 577	-16 439
ASP-NB	-17 566	-11 418	-17 545	-11 536	-16 028	-16 941
VRT(ASP-W)II	-17 601	-12 050	-17 185		-16 613	
VRT(ASP-W)III	-17 478	-11 663	-17 069	-11 814	-16 605	-16 357

^aRBDMC simulations with VRT(ASP-W)II all collapsed to the prism.

^bRBDMC simulations of VRT(ASP-W)III for the cyclic and book collapsed to the cage. Hence values of D_0 for these structures are not shown in the above table.

shown in Fig. 6. Indeed, because of this, it has been proposed as a prototype for analyzing hydrogen bonding in ice.²¹

As with the pentamer, it is well known that there is a large number of nearly isoenergetic ES's near the actual global minimum, the most relevant of which are shown in Fig. 6. The global minimum (equilibrium structure) on all potential surfaces examined here is the prism structure, shown in part (a). Table X shows that for all potentials, excluding the MP2 surface, the prism is significantly lower in energy than all other structures, with the cage structure being the closest to it. In the case of VRT(ASP-W)II and III, the prism structure is energetically even further from the cage than on the ASP-NB surface. VRT(ASP-W)II and III agree more closely with the MP2 surface in that they also predict the cyclic and book structures as the next two structures in terms of energetic ordering. ASP-NB predicts that the cyclic structure is higher in energy than the cage, most likely a flaw in the potential since high level *ab initio* calculations predict the

cyclic structure to be close to the prism and cage.⁵³ This is consistent with our findings for VRT(ASP-W)II and III.

RBDMC vibrationally averaged ground-state properties for all IPS's are shown in Table XI. There are some important observations to make about the predicted VGS. VRT(ASP-W)II predicts the prism as the VGS, whereas VRT(ASP-W)III correctly predicts the cage structure to be lowest in D_0 energy and the prism to be the next highest. Once again, this is surprising considering how similar the two IPS's were thought to be, and it again testifies to the "correctness" of the VRT(ASP-W)III IPS. SAPT5_s + NB(ASP) yields a value for D_0 that is once again within approximately 6.5% of that from VRT(ASP-W)III, but incorrectly predicts the book as the VGS. Efforts were made to constrain the simulations on SAPT5_s + NB(ASP) to the cage structure local minimum by using the cage configuration from VRT(ASP-W)III determined by ORIENT 4.4 as the starting configuration for the walkers. However, each attempt as such resulted in a prism structure with a value of D_0 of $-10\,713\text{ cm}^{-1}$. This seems to indicate that the SAPT5_s + NB(ASP) surface incorrectly predicts the ground-state structures of $(\text{H}_2\text{O})_6$. However, simulations with the "tuned" SAPT5_s + NB(ASP-T) yielded the correct VGS of the cage structure, and a value of D_0 within approximately +7% of that for VRT(ASP-W)III. Once again, this is very surprising considering the similar high degree of accuracy of both the SAPT5_s and SAPT5_s-T IPS families for cluster VGS up through the pentamer. The results for the hexamer once again illustrate the subtle but significant effect the fit-

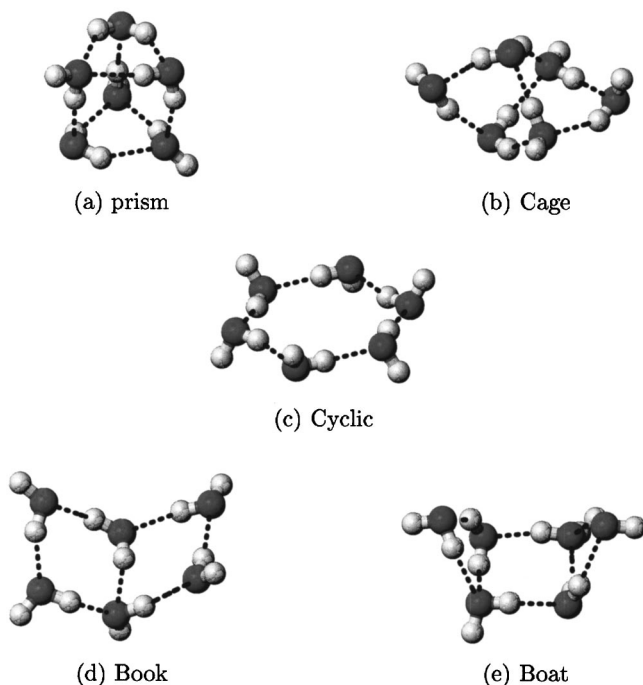


FIG. 6. The low-energy structures of the hexamer investigated in this study. Results for the boat structure are not presented in this paper but the structure is included in this figure for the sake of completeness.

TABLE XI. D_e and D_0 for $(\text{H}_2\text{O})_6$ minimum-energy structures. Listed in parentheses next to the name of each model is the different ground-state structure it predicts.

$(\text{H}_2\text{O})_6$ model	Global minimum	
	D_e (cm^{-1})	D_0 (cm^{-1})
MP2 (prism) ^a	-16 577	
ASP-NB (cage)	-17 545	-11 536
VRT(ASP-W)II (prism)	-17 601	-12 042
VRT(ASP-W)III (cage)	-17 478	-11 814
SAPT5 _s + NB(ASP) (book)		-11 095
SAPT5 _s + NB(ASP-T) (cage)		-10 999
PSPC (book)		-7 389
SPC/E (bird)		-12 994

^a D_0 for the MP2 surface was not calculated by Gregory and Clary (Ref. 28).

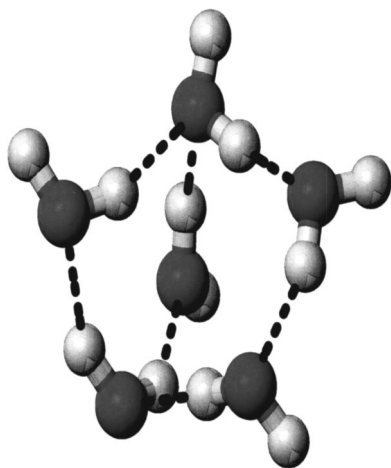


FIG. 7. Vibrationally averaged ground-state D_0 structure for SPC/E, named the "bird" structure.

ting of an IPS to spectroscopic data can have, and thus highlights the importance of continuing such efforts.

Also interesting to examine are the two structures predicted by the "bulk" potentials, PSPC and SPC/E. PSPC deviates significantly from experimental results by predicting a book VGS that is roughly 40% higher in energy than all other ground-state predictions. SPC/E exhibits a D_0 closer in energy to the gas phase IPS, but in keeping with its propensity for tetrahedral structure, it predicts a "birdlike" VGS, shown in Fig. 7. This structure is once again taken from a snapshot of a random walker during an RBDMC simulation. It resembles a distorted cyclic tetramer with the next two monomers up top sticking in and out of the $[OOOO]$ plane. Hence the bird has a mirror image plane that is defined by $[OOOO]$. Due to the effectiveness of SPC/E surface in simulating the bulk at standard conditions, as discussed below, this structure can be seen as a snapshot of what a hexamer instantaneously formed in the liquid would most probably look like.

The ground-state rotational constants for each potential are listed in Table XII. VRT(ASP-W)III, SAPT5s + NB(ASP-T) and ASP-NB are all in good agreement with the listed experimental results for $(\text{H}_2\text{O})_6$.

F. Discussion

The vibrationally averaged nearest-neighbor O–O distances for H_2O ground-state clusters calculated on several of the potentials are shown in Fig. 8. As the figure shows,

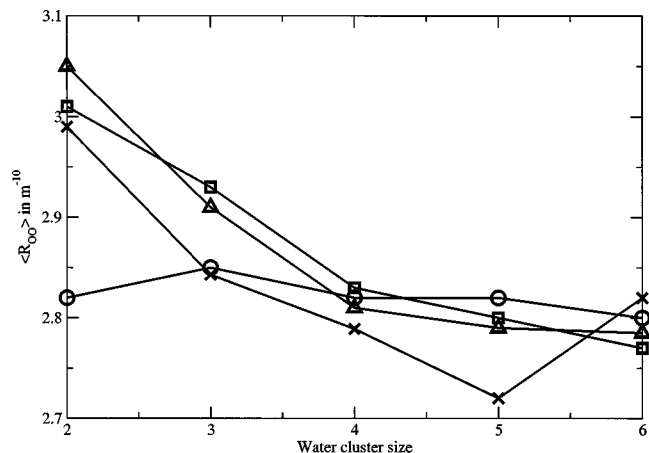


FIG. 8. Vibrationally averaged ground-state $\langle R_{OO} \rangle$ [Å] values for several potentials compared with experiment. ×'s correspond to experimental results, open squares to VRT(ASP-W)III, open triangles to ASP-NB (Ref. 28), and circles to SPC/E.

VRT(ASP-W)III performs very well as a model for higher order clusters. Upon examination of results for the pentamer and hexamer, it is clear that it represents a substantial improvement over VRT(ASP-W)II. As we have noted, this is surprising, considering that VRT(ASP-W)III represents a relatively minor refinement of version II in terms of dimer properties. However, this subtle refinement has major global consequences, since VRT(ASP-W)III is a much better model for the larger clusters. Hence continued fitting of ASP-W or other IPS's to larger spectroscopic data sets seems to be a worthwhile pursuit. Moreover, although SAPT5s + NB(ASP) describes clusters up through the pentamer quite well, tuning of an IPS to experimental data is clearly important since VRT(ASP-W)III and SAPT5s + NB(ASP-T) are the best models currently in existence for gas-phase clusters. The fact that the only many-body force present in VRT(ASP-W)III is induction supports the assertion that for gas-phase cluster calculations it seems reasonable to neglect all other many-body contributions (i.e., dispersion, exchange); hence the computational cost of including three-body exchange in VRT(ASP-W)III does not seem worthwhile. In addition, there does not exist a computationally cheap method for including three-body exchange with VRT(ASP-W)III. In SAPT5s + 3B, the three-body induction and exchange parameters were fit to the entire SCF nonadditive energy. Hence, due to correlations between parameters, one cannot simply insert the nonadditive exchange terms into a DMC

TABLE XII. $(\text{H}_2\text{O})_6$ vibrationally averaged rotational constants for ground-state structures.

$(\text{H}_2\text{O})_6$	VRT(ASP-W)II ^a	VRT(ASP-W)III ^b	SAPT5s + NB(ASP) ^c	SAPT5s + NB(ASP-T) ^b	PSPC ^c	SPC/E ^d	ASP-NB ^b	Expt. ^a
A (GHz)	1.678	2.107	1.83	2.08	1.789	1.581	2.136	2.164
B (GHz)	1.352	1.100	1.03	1.06	0.922	1.281	1.096	1.131
C (GHz)	1.266	1.025	0.74	0.94	0.673	1.053	1.043	1.069

^aPrism.

^bCage. Experimental results are from Ref. 21.

^cBook.

^dBird.

simulation with VRT(ASP-W)III, and would require a technique similar to what was used to calculate the $N > 3$ -body dispersion on the SAPT5 $_s$ + 3B potential surface.

In order to ascertain how VRT(ASP-W)III might perform in bulk simulations, it is instructive to compare VGS calculations between it, SPC/E and PSPC. SPC/E is the water model most widely in use and arguably the most accurate. It predicts a very accurate value for water surface tension at room temperature and above.⁴⁹ The surface tension is dependent upon the average value of the components of the pressure tensor, which is itself dependent upon the radial intermolecular force acting upon each monomer. As a result, surface tension can be viewed as a measure of the average force field experienced by the monomers.

In light of the above statement, RBDMC results from SPC/E most likely represent the highest probability structures for clusters that may form instantaneously in the bulk. As is shown by examining Figs. 5 and 7, in the SPC/E bulk, monomers have a strong tendency to form structures more closely resembling tetrahedrons. The fact that these VGS's differ so vastly from both experimental results and from those produced by VRT(ASP-W)III indicates that $(\text{H}_2\text{O})_6$ may not be the best prototype for investigating bulk water hydrogen bonding, as has been proposed in the literature.²¹ Indeed, although $(\text{H}_2\text{O})_6$ may have a value for $\langle R_{OO} \rangle$ and an O-H \cdots O bond angle that is close to bulk values, it clearly lacks the signature tetrahedral structure present in the bulk. Hence it appears that the continued experimental investigation of clusters larger than the hexamer is important in order to further elucidate structural details of the hydrogen bond network of the liquid and solid forms of water.

In addition, it is very interesting that for the pentamer and hexamer, SPC/E has a VGS energy that is lower than those from VRT(ASP-W)III, by 53 and 1180 cm^{-1} , respectively. Assuming this trend continues, and that for $N > 5$ -body clusters, SPC/E generally produces a lower D_0 , this implies that VRT(ASP-W)III is still missing long-range attractive correlations that are important for correctly simulating the structure of the bulk. This important implication will be investigated more thoroughly in a forthcoming paper (II).

Our investigations of PSPC are interesting but not quite as enlightening. The model is able to predict reasonably accurate ground-state structures, at least up to the pentamer. However, in terms of its energetics, it serves as a poor model in that it predicts values of D_0 that were consistently much higher than those of our IPS as well as the MP2 surface. This is most likely due to simplistic representation of molecular polarizabilities in terms of the constituent atomic ones. As a result, the model may not properly take into account cooperativity effects within clusters and thus underestimates the effects of induction. The fact that despite this, or maybe because of it, PSPC serves as a reasonable structural model for the liquid makes the idea of performing liquid simulations with VRT(ASP-W)III intriguing.

III. THE ROLE OF THREE-BODY DISPERSION

Considering the relatively high quality of the ASP-NB potential, it is of interest to perform a thorough analysis of

TABLE XIII. Effect of three-body dispersion on ES for the water trimer through hexamer. All values for D_e are in cm^{-1} , and the percentage of change is calculated relative to ASP-W.

$(\text{H}_2\text{O})_3$	ASP-NB	ASP-W	% change
(<i>uud</i>)	-5 626	-5 699	1.28
(<i>uuu</i>)	-5 297	-5 368	1.32
(<i>udud</i>)	-10 058	-10 083	0.25
(<i>uudd</i>)	-9 683	-9 715	0.33
(<i>uuud</i>)	-9 630	-9 666	0.37
C_5	-8 211	-7 310	12.33
Cage (6)	-13 179	-12 973	-1.59
Cyclic	-13 124	-13 119	-0.04
Envelope	-13 072	-13 152	0.61
Cage (7)	-12 868	-12 846	-0.16
Prism	-17 566	-17 649	0.47
Cage	-17 545	-17 276	-1.55
Book	-16 941		
Boat	-16 235	-16 393	0.96
Cyclic	-16 028	-16 072	0.31

the effects of the approximate form of the triple-dipole dispersion on energetic global minima and vibrational ground-state properties of water clusters. Although the effects are most likely quite small, inclusion of this three-body dispersion term greatly improved the performance of the ASP-W potential, as shown before by Gregory and Clary.²⁸

The simple Axilrod-Teller-Muto (ATM) expression for triple dipole dispersion is a simple isotropic approximation to the true tensorial form, detailed in Refs. 46 and 47. Its effect on ASP-W will be quantified through comparison of RBDMC and ORIENT 4.4 simulation results for the dimer through hexamer. Finally, some conclusions will be drawn as to its relevance to VRT(ASP-W)III.

A. Dispersion effects in ASP-W clusters

In order to quantify the dispersion effects in ASP-NB, the dimer through hexamer were simulated with ASP-W with converged induction. As mentioned in Sec. II, ASP-NB differs from ASP-W only in that it contains the ATM approximation for three-body dispersion. The effects on D_e are shown in Table XIII.

For the most part, the three-body dispersion effects on the interaction energy seem to be minimal, and fractional changes are on the order of 1% and less. The single structure that experiences significant energetic change is the C_5 tetramer, which is over 12% higher for ASP-W. This is undoubtedly due to the fact that the four possible triplets in the structure form obtuse triangles which have attractive three-body dispersion energies. The changes induced in the pentamer and hexamer are subtle, but significant as well. For the ASP-W pentamer, the energetic ordering has changed from the cage (6) to the envelope as the global minimum, followed by the cyclic structure, cage (6) and then cage (7). The reordering of the minima is possible because the minima all lie quite close to each other, so slight alterations of D_e can have significant effects. The changes for the hexamer are much less dramatic—the main feature to note is that the prism structure experiences attractive dispersion whereas the cage

TABLE XIV. Effects of three-body dispersion on VGS. Percent change is calculated from ASP-NB, relative to ASP-W.

ASP-W	D_0 (cm ⁻¹)	Structure	% change
(H ₂ O) ₃	-3 564	(<i>uud</i>)	-1.54
(H ₂ O) ₄	-6 593	(<i>udud</i>)	-2.75
(H ₂ O) ₅	-8 722	envelope	-3.66
(H ₂ O) ₆	-11 975	prism	-4.65

structure experiences a three-body repulsion. This causes the ASP-W structures to have a significantly larger energetic gap of 373 versus 21 cm⁻¹ for ASP-NB.

The results for the VGS for the trimer through hexamer are shown in Table XIV, and the corresponding rotational constants in Table XV. As Table XIV indicates, the overall effect of the dispersion term on the VGS energy is quite small—at most a couple of percent, in the case of (H₂O)₅. Table XV shows that the effect on ground-state structural properties is much stronger. Structures for (D₂O)₃, (D₂O)₄, and (D₂O)₅ were all determined experimentally to be cyclic, corresponding to oblate tops. ASP-W consistently overestimates the A rotational constant, and in the case of (D₂O)₅, the envelope emerges as the VGS. Due to the larger energy gaps between the prism and cage structures, the ASP-W (H₂O)₆ VGS is the prism. We have not attempted to reproduce Gregory and Clary's results for ASP-NB, but according to Ref. 28, it does an excellent job of ground-state structural prediction. It yields perfect oblate tops for (D₂O)₃, (D₂O)₄, and (D₂O)₅, and rotational constants for the (H₂O)₆ cage that are very close to experimental results. Nonetheless, the results seem somewhat unreasonable considering the small percent of the interaction energy that corresponds to dispersion. Certainly it seems plausible that the addition of dispersion may cause (D₂O)₃ and (D₂O)₄ to become more oblate, and thus for (D₂O)₅ and (D₂O)₆ to match experiments more closely, but the values of A obtained for the ASP-W (D₂O)₃ and (D₂O)₄ clusters are close to 20% greater than those reported in Ref. 28. These changes appear to be too great to be able to be corrected by Axilrod–Teller dispersion. Verifying their calculations is not worthwhile at this point, but it seems that those results should be viewed with caution.

B. Discussion

Despite the fact that three-body dispersion may have resulted in significant changes in some of the ASP-W cluster properties, it does not seem worthwhile to quantify the ef-

TABLE XV. Ground-state rotational constants for the trimer through hexamer.

	ASP-W			
	(D ₂ O) ₃	(D ₂ O) ₄	(D ₂ O) ₅ ^a	(H ₂ O) ₆ ^b
A (GHz)	6.119	3.248	1.864	1.634
B (GHz)	5.147	2.818	1.634	1.374
C (GHz)	2.904	1.574	0.925	1.266

^aEnvelope structure.

^bPrism structure.

fects it would have on VRT(ASP-W)III. The potential minima in VRT(ASP-W)III are not spaced as close together as those in ASP-W, so it is not expected that ATM three-body dispersion could cause a reordering of energetic structures. For example, for the VRT(ASP-W)III pentamer, the smallest energy difference in D_e is between envelope and cyclic structures, which are 205 cm⁻¹ apart. This corresponds to approximately 1.55% of the value of D_e for the envelope, which according to Table XIII would be the very upper limit for the ATM effects.

It is important to note again that the ATM three-body dispersion is isotropic and consequently is less accurate than a tensorial representation of the triple dipole interaction. The effect of using a more accurate triple-dipole dispersion term can be estimated if we view the tensorial interaction as the inclusion of additional degrees of freedom over an isotropic representation. Additional degrees of freedom would allow a water cluster to “relax” energetically more easily if a given interaction were repulsive, and they would allow the cluster to enhance the interaction if it were attractive. Thus it follows that the repulsive three-body interactions in such a tensorial representation would be smaller than those of the ATM approximation, and the attractive interactions would be larger. Hence it is clear that further energetic reordering of local minima will take place, especially in clusters where the local minima are nearly isoenergetic, such as with the pentamer, hexamer, and larger clusters. Regardless, as stated in the Introduction, three-body exchange is significantly larger in magnitude than three-body dispersion. As a result, it is very important to include both types of forces in order to quantify the overall three-body effects on an IPS.

IV. DISCUSSION

We have developed² a new water dimer potential [VRT(ASP-W)III], from a fit to (D₂O)₂ spectroscopic data with induction as the only many-body force included. It predicts quite accurate ground-state properties for the water dimer through hexamer, and can thus serve as a good model for dynamics of larger clusters. This is an important step for the calculation of condensation properties, which requires accurate evaluation of the cluster free-energy surface (see, for example, Ref. 54).

The improvement of VRT(ASP-W)III relative to version II is significant, and it is notable that the addition of just a few additional transitions greatly improved structural predictions for the pentamer and hexamer. The next test of VRT(ASP-W)III will be to employ it in actual liquid simulations. Whereas the proper inclusion of induction has been shown to be sufficient for simulations of clusters, there is a good chance that it is not sufficient to model the long-range correlations present in the liquid. It is quite possible that other many-body effects, viz. dispersion and exchange, may prove important for simulation of the bulk. This is examined in a forthcoming paper.

ACKNOWLEDGMENTS

This work was supported by the Experimental Physical Chemistry Program of the National Science Foundation. The

authors would like to thank Mac Brown for initial help with writing the DMC code, and Krzysztof Szalewicz and Robert Bukowski for use of their SAPT potential code and for many helpful discussions. They would also like to thank Krzysztof Szalewicz and Robert Bukowski, as well as Anthony Stone for a critical review of the manuscript.

- ¹F. N. Keutsch and R. J. Saykally, Proc. Natl. Acad. Sci. U.S.A. **98**, 10533 (2001).
- ²N. Goldman, R. S. Fellers, M. G. Brown, L. B. Braly, C. J. Keoshian, C. Leforestier, and R. J. Saykally, J. Chem. Phys. **116**, 10148 (2002).
- ³G. C. Groenenboom, E. Mas, R. Bukowski, K. Szalewicz, P. E. S. Wormer, and A. van der Avoird, Phys. Rev. Lett. **84**, 4072 (2000).
- ⁴G. C. Groenenboom, P. E. S. Wormer, A. van der Avoird, E. Mas, R. Bukowski, and K. Szalewicz, J. Chem. Phys. **113**, 6702 (2000).
- ⁵C. Millot, J. C. Soetens, M. T. C. Martins-Costa, M. P. Hodges, and A. J. Stone, J. Phys. Chem. A **102**, 754 (1998).
- ⁶E. M. Mas, R. A. Bukowski, K. A. Szalewicz, G. C. Groenenboom, P. E. S. Wprmer, and A. van der Avoird, J. Chem. Phys. **113**, 6687 (2000).
- ⁷E. M. Mas, R. Bukowski, and K. Szalewicz, J. Chem. Phys. **118**, 4386 (2003).
- ⁸M. P. Hodges, A. J. Stone, and S. S. Xantheas, J. Phys. Chem. A **101**, 9163 (1997).
- ⁹L. Ojamäe and K. Hermansson, J. Phys. Chem. **98**, 4271 (1994).
- ¹⁰C. Millot and A. J. Stone, Mol. Phys. **77**, 439 (1992).
- ¹¹R. J. Saykally and G. A. Blake, Science **259**, 1570 (1993).
- ¹²L. B. Braly, J. D. Cruzan, K. Liu, R. S. Fellers, and R. J. Saykally, J. Chem. Phys. **112**, 10293(2000).
- ¹³L. B. Braly, K. Liu, M. G. Brown, F. N. Keutsch, R. S. Fellers, and R. J. Saykally, J. Chem. Phys. **112**, 10314 (2000).
- ¹⁴K. L. Busarow, R. C. Cohen, G. A. Blake, K. B. Laughlin, Y. T. Lee, and R. J. Saykally, J. Chem. Phys. **90**, 3937 (1989).
- ¹⁵R. S. Fellers, C. Leforestier, L. Braly, M. G. Brown, and R. J. Saykally, Science **284**, 945 (1999).
- ¹⁶J. K. Gregory and D. C. Clary, J. Chem. Phys. **103**, 8924 (1995).
- ¹⁷G. Chalasinski, M. M. Szczesniak, P. Cieplak, and S. Scheiner, J. Chem. Phys. **94**, 2873 (1991).
- ¹⁸P. L. Geissler, C. D. Dellago, D. Chandler, J. Hutter, and M. Parrinello, Science **291**, 2121 (2001).
- ¹⁹K. Liu, J. G. Loeser, M. J. Elrod, B. C. Host, J. A. Rzepiela, and R. J. Saykally, J. Am. Chem. Soc. **116**, 3507 (1994).
- ²⁰K. Liu, J. D. Cruzan, and R. J. Saykally, Science **271**, 929 (1996), and references therein.
- ²¹K. Liu, M. G. Brown, C. Carter, R. J. Saykally, J. K. Gregory, and D. C. Clary, Nature (London) **381**, 501 (1996).
- ²²K. Liu, M. G. Brown, J. D. Cruzan, and R. J. Saykally, Science **271**, 62 (1996).
- ²³K. Liu, M. G. Brown, and R. J. Saykally, J. Phys. Chem. A **101**, 8995 (1997).
- ²⁴N. Pugliano and R. J. Saykally, Science **257**, 1937 (1992).
- ²⁵J. Gregory and D. C. Clary, Chem. Phys. Lett. **228**, 547 (1994).
- ²⁶J. K. Gregory and D. C. Clary, J. Chem. Phys. **102**, 7817 (1995).
- ²⁷J. Gregory and D. C. Clary, J. Chem. Phys. **103**, 8924 (1995).
- ²⁸J. K. Gregory and D. C. Clary, J. Phys. Chem. **100**, 18014 (1996).
- ²⁹J. K. Gregory and D. C. Clary, J. Chem. Phys. **105**, 6626 (1996).
- ³⁰J. K. Gregory, D. C. Clary, K. Liu, M. G. Brown, and R. J. Saykally, Science **275**, 814 (1997).
- ³¹M. Quack and M. A. Suhm, Mol. Phys. **69**, 79' (1990).
- ³²M. Quack and M. A. Suhm, Chem. Phys. Lett. **183**, 187 (1991).
- ³³M. Quack and M. A. Suhm, J. Chem. Phys. **95**, 28 (1991).
- ³⁴W. Klopper, M. Quack, and M. A. Suhm, J. Chem. Phys. **108**, 10096 (1998).
- ³⁵M. Quack, R. Stohner, and M. A. Suhm, J. Mol. Struct. **599**, 381 (2001).
- ³⁶J. B. Anderson, J. Chem. Phys. **63**, 1499 (1975).
- ³⁷J. B. Anderson, J. Chem. Phys. **65**, 4121 (1976).
- ³⁸M. A. Suhm and R. O. Watts, Phys. Rep. **204**, 293 (1991).
- ³⁹V. Buch, J. Chem. Phys. **97**, 726 (1992).
- ⁴⁰P. Sandler, J. O. Jung, M. M. Szczesniak, and V. Buch, J. Chem. Phys. **101**, 1378 (1994).
- ⁴¹M. W. Severson and V. Buch, J. Chem. Phys. **111**, 10866 (1999).
- ⁴²D. Blume and K. B. Whaley, J. Chem. Phys. **112**, 2218 (2000).
- ⁴³H. J. C. Berendsen, J. R. Grigera, and T. P. Straatsma, J. Phys. Chem. **91**, 6269 (1987).
- ⁴⁴D. N. Bernardo, Y. Ding, K. Krogh-Jespersen, and R. M. Levy, J. Phys. Chem. **98**, 4180 (1994).
- ⁴⁵A. J. Stone, A. Dullweber, O. Engkvist, E. Frascini, M. P. Hodges, A. W. Meredith, P. L. A. Popelier, and D. J. Wales, *Orient: A Program for Studying Interactions Between Molecules, Version 4.4* (University of Cambridge, Cambridge, 2000), <http://fandango.ch.cam.ac.uk/>
- ⁴⁶B. M. Axilrod and E. Teller, J. Chem. Phys. **11**, 299 (1943).
- ⁴⁷Y. Muto, Proc. Phys. Math. Soc. Jpn. **17**, 629 (1943).
- ⁴⁸E. M. Mas, R. Bukowski, and K. Szalewicz, J. Chem. Phys. **118**, 4404 (2003).
- ⁴⁹J. A. Alejandre, D. J. Tildesley, and G. A. Chapela, J. Chem. Phys. **102**, 4574 (1995).
- ⁵⁰L. X. Dang and T.-M. Chang, J. Chem. Phys. **106**, 8149 (1997).
- ⁵¹F. Keutsch, J. Cruzan, and R. J. Saykally, Chem. Rev. **107**, 2533 (2003).
- ⁵²M. G. Brown, M. R. Viant, R. P. McLaughlin, C. J. Keoshian, E. Michael, J. D. Cruzan, and R. J. Saykally, J. Chem. Phys. **111**, 7789 (1999).
- ⁵³K. Kim, K. D. Jordon, and T. S. Zwier, J. Am. Chem. Soc. **115**, 11568 (1994).
- ⁵⁴S. M. Kathman, G. K. Schenter, and B. C. Garrett, J. Chem. Phys. **111**, 4688 (1999).
- ⁵⁵L. B. Braly, Ph.D. thesis, University of California, Berkeley, 1999.
- ⁵⁶S. Xantheas and T. H. Dunning, J. Chem. Phys. **99**, 8774 (1993).